

CLIMP: Contrastive Language-Image Mamba Pretraining

Nimrod Shabtay^{1,2}, Itamar Zimerman², Eli Schwartz¹, Raja Giryes²

¹IBM Research, ²Tel-Aviv University

Abstract

Contrastive Language-Image Pre-training (CLIP) relies on Vision Transformers whose attention mechanism is susceptible to spurious correlations, and scales quadratically with resolution. To address these limitations, We present CLIMP, the first fully Mamba-based contrastive vision-language model that replaces both the vision and text encoders with Mamba. The new architecture encodes sequential structure in both vision and language, with VMamba capturing visual spatial inductive biases, reducing reliance on spurious correlations and producing an embedding space favorable for cross-modal retrieval and out-of-distribution robustness-surpassing OpenAI’s CLIP-ViT-B by 7.5% on ImageNet-O. CLIMP naturally supports variable input resolutions without positional encoding interpolation or specialized training, achieving up to 6.6% higher retrieval accuracy at 16 \times training resolution while using 5 \times less memory and 1.8 \times fewer FLOPs. The autoregressive text encoder further overcomes CLIP’s fixed context limitation, enabling dense captioning retrieval. Our findings suggest that Mamba exhibits advantageous properties for vision-language learning, making it a compelling alternative to Transformer-based CLIP.

1 Introduction

Contrastive Language-Image Pre-training (CLIP) proposed by Radford et al. (2021) is a fundamental approach for learning transferable visual representations through natural language supervision. By aligning image and text embeddings in a shared latent space, CLIP enables zero-shot transfer across a range of downstream tasks. However, the Vision Transformer (ViT) (Dosovitskiy et al., 2021) backbone commonly employed in CLIP exhibits quadratic computational complexity with respect to sequence length, posing challenges when processing high-resolution images. Moreover, the pairwise token interactions in self-attention can

be susceptible to spurious correlations (Zhou and Zhu, 2025; Tamayo-Rousseau et al., 2025), leading to fragile representations under distribution shift. In contrast, Mamba’s recurrent state-space formulation aggregates context through selective state updates rather than explicit pairwise comparisons, yielding representations with tighter cross-modal alignment while resisting collapse toward generic features - geometric properties that translate to improved retrieval and robustness.

Mamba (Gu and Dao, 2024), which is a state-space model (SSM), have shown promising results as an alternative to Transformers in sequence modeling. It achieves sub-quadratic complexity in sequence length L during training and constant-time complexity during inference, with these efficiency benefits becoming more pronounced in long-context scenarios. These properties make Mamba an attractive backbone for vision-language tasks requiring long-context processing such as dense captioning.

In the vision domain, adaptations such as Vision Mamba (Vim) (Zhu et al., 2024), Simba (Patro and Agneeswaran, 2024) and VMamba (Liu et al., 2024) have applied state space models to image understanding tasks with encouraging results. Beyond computational considerations, which allow high resolution processing, these models introduce spatial inductive biases that differ from the pairwise token interactions characteristic of self-attention. Prior work has shown that such spatial bias benefits vision tasks by enabling more robust (Malik et al., 2025; Du et al., 2024) and sample-efficient learning (d’Ascoli et al., 2021)—properties that ViTs lack. However, the integration of Mamba-based vision encoders into contrastive vision-language frameworks remains relatively unexplored. Indeed, prior work (Huang et al., 2024) has investigated contrastive pretraining of a combination of Mamba and transformers models for the vision and language towers. However, their evaluation is limited and does not explore a fully SSM-based architecture.

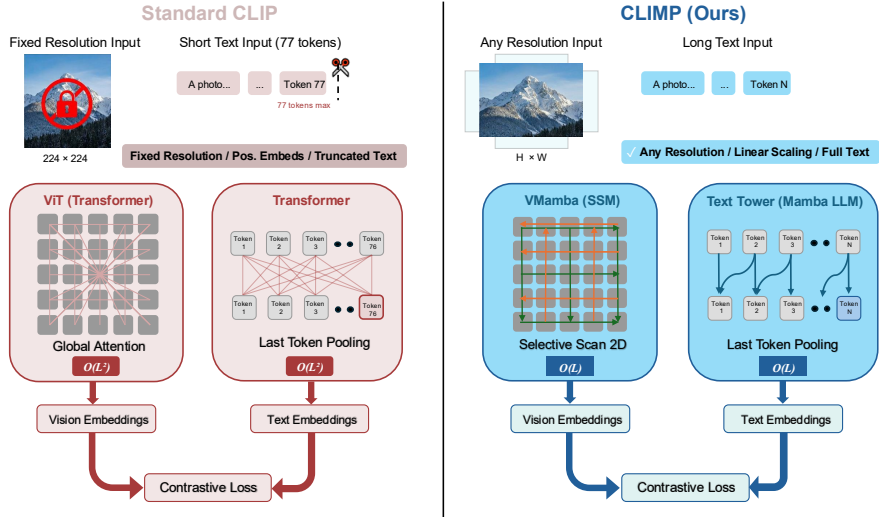


Figure 1: **CLIP vs. CLIMP.** By replacing Transformer encoders with Mamba-based models, CLIMP achieves sub-quadratic $O(L)$ complexity instead of quadratic $O(L^2)$, while removing the fixed resolution and 77-token text limitations inherent to standard CLIP.

We empirically confirm that VMamba’s spatial inductive bias transfers to the vision-language setting, enabling improved sample efficiency and robustness (Section 4.5).

In this work, we present Contrastive Language-Image Mamba Pretraining (CLIMP), a fully Mamba-based vision-language model that replaces both the vision and text encoders with state-space architectures within the CLIP framework. We pair VMamba (Liu et al., 2024) as the vision encoder with Mamba-1 (Gu and Dao, 2024) or Mamba-2 (Dao and Gu, 2024) language models as text encoders, creating the first end-to-end SSM-based contrastive vision-language model.

Our main contributions are: (1) We present CLIMP, the first fully Mamba-based CLIP model, integrating VMamba for vision and Mamba LLMs for text, yielding representations with tighter cross-modal alignment. (2) CLIMP achieves superior OOD robustness, claiming the top positions on average across ImageNet variants. On ImageNet-O, it surpasses OpenAI’s CLIP-ViT-B/16 trained on LAION-2B - a dataset $167\times$ larger than ours. (3) CLIMP naturally supports variable input resolutions without complex positional encoding schemes or dedicated training, with significantly lower memory and compute overhead. At high resolutions, it maintains strong retrieval performance while transformer baselines degrade significantly.

Our findings suggest that state space models represent a promising direction for vision-language learning, offering compelling advantages for retrieval, high-resolution processing, computational efficiency, and robustness to distribution shifts.

2 Related Work

Contrastive Vision-Language Learning. CLIP (Radford et al., 2021) marked a paradigm shift in vision-language learning by demonstrating that models trained on large-scale image-text pairs can achieve remarkable zero-shot transfer capabilities. It learns a joint embedding space where semantically similar images and texts are mapped close together, enabling open-vocabulary recognition without task-specific fine-tuning. Following CLIP’s success, numerous works have sought to improve upon its framework. OpenCLIP (Cherti et al., 2023) provides an open-source reproduction with reproducible scaling laws, training models on datasets such as LAION-400M (Schuhmann et al., 2021) and LAION-2B (Schuhmann et al., 2022). SigLIP (Zhai et al., 2023) replaces the softmax-based contrastive loss with a pairwise sigmoid loss, improving memory efficiency and enabling training with smaller batch sizes. EVA-CLIP (Sun et al., 2023) enhances the training recipe with stronger vision and text encoders, achieving state-of-the-art zero-shot performance. ALIGN (Jia et al., 2021) scaled the training data with noisy image-text pairs. More recent efforts include MetaCLIP (Xu et al., 2024), which introduces data curation algorithms for balanced training distributions, and SigLIP 2 (Tschannen et al., 2025), which adds captioning-based pretraining and self-supervised losses.

Despite these advances, all existing CLIP variants rely on Transformer-based vision encoders, predominantly the Vision Transformer (ViT) (Dosovitskiy et al., 2021). While ViT has proven highly

effective, its quadratic complexity with respect to sequence length poses challenges for high-resolution image processing. Scaling ViT to higher resolutions requires substantial computational resources and for a dynamic resolution processing ViT requires a specialized positional encoding schemes such as RoPE (Su et al., 2024) or dedicated training scheme (Beyer et al., 2023). Furthermore, studies have shown that CLIP’s robustness to distribution shifts, while impressive on ImageNet variants (Taori et al., 2020; Fang et al., 2022), may be overestimated when evaluated on datasets specifically designed to probe spurious correlations (Li et al., 2024b). These limitations motivate our exploration of alternative vision backbones that offer improved efficiency at high resolutions while enhancing robustness.

CLIMP is the first work to systematically investigate Mamba vision encoders within the CLIP framework. Replacing ViT with VMamba, addresses the computational bottleneck of high-resolution processing, and enables a dynamic resolution processing that achieves improved zero-shot performance and improved robustness to distribution shifts.

State Space Models (SSMs) for Vision. SSMs have emerged as a promising alternative to Transformers for sequence modeling. The Mamba architecture (Gu and Dao, 2024) introduced a selective mechanism that makes SSM parameters input-dependent, enabling content-aware reasoning with linear complexity. Mamba-2 (Dao and Gu, 2024) further refined this approach through the State Space Duality (SSD) framework, establishing theoretical connections between SSMs and attention while achieving 2-8 \times speedups.

Adapting Mamba for vision tasks presents unique challenges, as images are inherently 2D and lack the sequential structure of language. Vision Mamba (Vim) (Zhu et al., 2024) addresses this by introducing bidirectional scanning with position embeddings, achieving competitive performance on ImageNet classification. SiMBA (Patro and Agneeswaran, 2024) addresses the stability issues of Mamba when scaling to large vision networks by introducing Einstein FFT for channel modeling, achieving state-of-the-art SSM performance on ImageNet and multiple time series benchmarks. VMamba (Liu et al., 2024) proposes the 2D Selective Scan (SS2D) module, which unfolds image patches along four traversal paths to capture global context while maintaining linear complexity. This cross-scan enables each patch to integrate information from all spatial directions, effectively estab-

lishing global receptive fields. Subsequent works have extended visual SSMs to various domains, including medical image segmentation (Ruan and Xiang, 2024), video understanding (Li et al., 2024a), and point cloud processing (Zhang et al., 2024). Recent studies have also begun exploring the robustness properties of visual SSMs. Du et al. (2024); Malik et al. (2025) investigate the robustness of visual SSMs for image classification, finding that Mamba-based architectures exhibit different failure modes compared to ViTs under adversarial perturbations and distribution shifts. These findings suggest that the inductive biases of SSMs may offer complementary advantages to attention-based models in terms of robustness.

While prior work has established the effectiveness of visual SSMs for classification tasks, their potential for vision-language learning remains largely unexplored. CLIMP bridges this gap by integrating VMamba into the CLIP framework, demonstrating that Mamba-based vision encoders can learn effective multimodal representations. Our experiments reveal that the architectural properties of SSMs—particularly their implicit handling of positional information through scanning patterns—enable native resolution flexibility and contribute to improved robustness on out-of-distribution benchmarks.

3 CLIMP

Motivation. Mamba has been shown to offer several advantages over attention models, including (1) improved long-context efficiency and scalability, (2) enhanced robustness, and (3) positional awareness. To better understand the suitability of Mamba models for CLIP, we focus on *inductive bias*, which is an important factor for sample-efficiency, out-of-distribution generalization, and representational capacity.

We study inductive bias through both empirical and analytical analyses. Empirically, we present positive results in Section 4.5.1 using synthetic tasks executed in controlled environments. Analytically, prior work has provided evidence that state-space layers exhibit inductive bias toward smoothness and locality compared to Transformers (Zimerman and Wolf, 2024). However, these analyses do not directly extend to selective SSMs, where the dynamics depend on the input. For Mamba-2, certain aspects of the inductive bias are easier to characterize. In particular, the recurrent update uses a per-step transition matrix \bar{A} parameterized as a diagonal matrix with scalar entries, $\bar{A} = \lambda I$. Thus,

Vision Tower	Text Tower	Zero-shot Classification		Zero-shot Retrieval	
		Acc@1	Acc@5	IR@5	TR@5
FlexViT-B/16	LLaMA-3.2	26.3	57.4	62.4	72.3
NaFlex-B/16	LLaMA-3.2	26.1	56.6	61.5	73.3
ViT-B/16	LLaMA-3.2	27.3	56.4	62.8	72.9
RoPE-ViT-B/16	LLaMA-3.2	27.3	59.0	63.4	72.9
CLIMP (VMamba-B)	Mamba-2	26.9	59.0	65.2	75.3
CLIMP (VMamba-B)	Mamba-1	29.6	58.5	65.5	77.0

Table 1: **CLIP-Benchmark Results.** Zero-shot classification and retrieval performance on 31 datasets. We evaluate two CLIMP variants with different text encoders: Mamba-2 and Mamba-1. Both CLIMP variants achieve the top two positions on retrieval metrics (Image Recall (IR) and Text Recall (TR), outperforming all transformer baselines. For classification, the Mamba-1 variant achieves the best Acc@1, while the Mamba-2 variant ties for the best Acc@5.

under standard stability conditions, the influence of a state k steps in the past on the current token decays proportionally to λ^k , resulting in exponentially decreasing contributions from distant states, which encourages an inductive bias toward locality and smoothness. By replacing Transformers entirely with Mamba, CLIMP achieves sub-quadratic memory complexity in both modalities while maintaining improved representation quality.

3.1 Preliminaries

State Space Models (SSMs) map an input sequence $x(t) \in \mathbb{R}$ to an output $y(t) \in \mathbb{R}$ through a latent state $h(t) \in \mathbb{R}^N$, according to the following dynamics:

$$h'(t) = \mathbf{A}h(t) + \mathbf{B}x(t), \quad y(t) = \mathbf{C}h(t) + \mathbf{D}x(t),$$

where $\mathbf{A} \in \mathbb{R}^{N \times N}$, $\mathbf{B} \in \mathbb{R}^{N \times 1}$, $\mathbf{C} \in \mathbb{R}^{1 \times N}$, and $\mathbf{D} \in \mathbb{R}$ are learnable parameters. For discrete sequences, the system is discretized using step size Δ :

$$h_t = \bar{\mathbf{A}}h_{t-1} + \bar{\mathbf{B}}x_t, \quad y_t = \mathbf{C}h_t + \mathbf{D}x_t,$$

where $\bar{\mathbf{A}}$ and $\bar{\mathbf{B}}$ are the discretized parameters. Mamba (Gu and Dao, 2024) introduces input-dependent selection by making \mathbf{B} , \mathbf{C} , and Δ functions of input x_t , enabling content-aware reasoning with linear complexity. Mamba-2 (Dao and Gu, 2024) further constrains \mathbf{A} to a scalar times identity matrix, recasting computation as structured matrix multiplications to gain 2-8 \times speedup.

3.2 Model Architecture

CLIMP follows CLIP’s dual-encoder architecture, mapping images and text into a shared embedding space. Crucially, both encoders are Mamba-based, offering consistent sub-quadratic memory scaling across modalities. An overview is shown in Figure 1.

Vision Encoder. We adopt VMamba (Liu et al., 2024) as the vision encoder. Given an input image $\mathbf{I} \in \mathbb{R}^{H \times W \times 3}$, we divide it into non-overlapping patches of size $P \times P$ and project them into patch embeddings processed through Visual State-Space (VSS) blocks utilizing the SS2D cross-scan mechanism. The hierarchical structure progressively downsamples feature maps through patch merging, with final features mapped to the shared embedding space via a learned projection W_v .

A key advantage is the implicit handling of spatial relationships through scanning patterns, providing a favorable spatial inductive bias (see Section A.5), allowing CLIMP to process variable input resolutions without positional encoding interpolation, specialized schemes like RoPE (Su et al., 2024), or complex training procedures like FlexViT (Beyer et al., 2023) and NaFlex (Dehghani et al., 2024).

Text Encoder. We employ pretrained Mamba LLMs as text encoders: Mamba-1 (Gu and Dao, 2024) (1.4B parameters) and Mamba-2 (Dao and Gu, 2024) (1.3B parameters). While both share the selective state-space foundation, Mamba-2 introduces structured state-space duality (SSD) enabling more efficient computation. Unlike transformers with mature bidirectional encoders (Devlin et al., 2019; Liu et al., 2019), Mamba models are autoregressive by design and we further analyze the role of the text tower in Table 8.

Given tokenized input $\mathbf{T} = [t_1, t_2, \dots, t_L]$ with padding mask $\mathbf{m} \in \{0, 1\}^L$, we extract the hidden state at the last non-padding token as the text representation:

$$\mathbf{t}_{\text{raw}} = \mathbf{H}_k, \quad \text{where } k = \max\{i : m_i = 0\} \quad (1)$$

where $\mathbf{H} = [\mathbf{h}_1, \mathbf{h}_2, \dots, \mathbf{h}_L]$ denotes hidden states from the last Mamba layer. This last-token pooling is well-suited for Mamba’s causal formulation,

where each \mathbf{h}_t is computed recurrently, making the last token the only position with full context access. It also enables dense captioning retrieval beyond CLIP’s 77-token limit (Section A.4). The representation is projected to the shared embedding space via W_t .

4 Results

Motivated by the advantages of Mamba architectures over transformer models, we evaluate CLIMP to assess whether its design yields improved retrieval, robustness, generalization, and overall performance. We begin with standard CLIP benchmarks for classification and retrieval (Section 4.1), then evaluate out-of-distribution robustness (Section 4.2) and resolution flexibility (Section 4.3). We further test robustness to extended text inputs via dense captioning retrieval (Section 4.4). Finally, we provide analysis including qualitative results, representational geometry, memory and FLOPs efficiency, scaling behavior, and the role of spatial inductive bias in VMamba’s performance (Section 4.5).

Experimental Setup. We train all models on CC12M (Changpinyo et al., 2021) for 10 epochs at 224×224 resolution using AdamW with cosine learning rate schedule (peak LR 5×10^{-5}), batch size 2048, and projection dimension 768. All vision encoders are base-sized (~ 86 M parameters) initialized from ImageNet-1K (Deng et al., 2009). For CLIMP, we use VMamba-B (Liu et al., 2024) as vision encoder with two text encoder variants: Mamba-1 (1.4B) (Gu and Dao, 2024) and Mamba-2 (1.3B) (Dao and Gu, 2024). We compare against three transformer baselines, all using LLaMA-3.2-1B (Touvron et al., 2023) (1.23B) as text encoder: RoPE-ViT (Heo et al., 2024), which uses Rotary Position Embeddings for resolution-flexible encoding; FlexViT (Beyer et al., 2023), trained with randomized patch sizes for arbitrary resolution inference; and NaFlex-ViT (Dehghani et al., 2024), which processes native resolutions without resizing via sequence packing.

4.1 CLIP-Benchmarks Results

We evaluate on CLIP-Benchmark (Cherti and Beaumont, 2025) (31 datasets for zero-shot classification and retrieval). Table 1 presents our main findings. Both CLIMP variants achieve top retrieval performance: Mamba-1 leads with 65.5% image and 77.0% text recall, outperforming the best transformer baseline (RoPE-ViT) by +2.1%

and +4.1% respectively. For classification, CLIMP-Mamba-1 achieves the top top-1 accuracy (29.6%, +2.3% over baselines), while CLIMP-Mamba-2 ties for best top-5 accuracy (59.0%).

These results demonstrate that fully SSM-based architectures can match or exceed transformers on vision-language tasks, with significant retrieval gains stemming from Mamba’s learned representations, which are better suited for retrieval and OOD tasks (see Section 4.5 for analysis).

4.2 OOD Robustness

We evaluate out-of-distribution robustness on five ImageNet variants: ImageNet-V2 (Recht et al., 2019), ImageNet-R (Hendrycks et al., 2020), ImageNet-A (Hendrycks et al., 2021), ImageNet-O (Hendrycks et al., 2021), and ImageNet-Sketch (Wang et al., 2019), testing natural distribution shift, renditions, adversarial examples, OOD detection, and sketch representations respectively.

As shown in Table 2, both CLIMP variants achieve the top two average robustness scores across all five benchmarks, with Mamba-1 leading at 35.2% top-1 and 64.3% top-5, followed by Mamba-2 at 34.8% and 63.7%. Both outperform the best transformer baseline (RoPE-ViT) by +2.0%/+1.6% on top-1 and +2.2%/+1.6% on top-5 average accuracy.

The most striking results are on ImageNet-O, where both CLIMP variants dramatically outperform all transformer baselines. Mamba-2 achieves 49.8% top-1 accuracy, followed by Mamba-1 at 48.1% - surpassing the best transformer baseline by +9.7% and +8.0% respectively. Remarkably, both variants surpass CLIP-ViT-B-16 (Radford et al., 2021) (42.3%)¹ trained on LAION-2B (Schuhmann et al., 2022), a dataset approximately 167× larger than CC12M (Changpinyo et al., 2021). This suggests that architectural inductive biases may be more critical for OOD robustness than training data scale alone, consistent with our geometric analysis 4.5.3 showing that CLIMP’s fewer generic embeddings leads to less reliance on spurious feature correlations that typically fail under distribution shift.

Both CLIMP variants also achieve the top two positions on ImageNet-V2 (+3.1%/+2.6% over the best transformer). On ImageNet-R and ImageNet-A, RoPE-ViT performs best, though CLIMP remains competitive within 1–2%. This aligns with prior findings that SSMs and transformers exhibit different failure modes under distribution shift (Du

¹Taken from: OpenCLIP Results

Vision Tower	Text Tower	IN-V2	IN-R	IN-A	IN-O	Sketch	Avg
FlexViT-B/16	LLaMA-3.2	32.8/62.5	45.4/74.3	13.2/41.2	38.1/68.2	24.6/50.0	30.8/59.2
NaFlex-B/16	LLaMA-3.2	31.4/60.5	44.8/72.5	12.0/36.0	38.5/67.6	23.5/49.1	30.0/57.1
ViT-B/16	LLaMA-3.2	30.0/57.5	42.9/69.7	13.9/37.6	27.7/55.8	21.7/46.1	27.2/53.3
RoPE-ViT-B/16	LLaMA-3.2	34.4/65.4	47.8/76.0	16.3/46.3	40.1/69.9	27.4/53.1	33.2/62.1
CLIMP (VMamba-B)	Mamba-2	<u>37.0/67.6</u>	<u>46.6/74.5</u>	<u>15.6/45.5</u>	49.8/77.0	27.0/54.2	<u>34.8/63.7</u>
CLIMP (VMamba-B)	Mamba-1	37.5/68.4	46.2/74.5	15.5/45.3	<u>48.1/78.8</u>	27.5/54.4	35.2/64.3

Table 2: **Out-of-distribution robustness.** Evaluation on ImageNet variant datasets, reporting top-1/top-5 accuracy. Both CLIMP variants achieve the top two average scores, with particularly strong gains on ImageNet-O (+9.7%/+8.0% over the best transformer) and ImageNet-V2 (+3.1%/+2.6%).

Vision	Text	Acc@1/Acc@5			IR@5/TR@5		
		224	320	384	224	320	384
FlexViT	LLaMA	26.3/57.3	26.1/57.3	25.9/56.9	62.4/72.3	63.5/74.3	63.6/75.0
NaFlex	LLaMA	26.1/56.6	25.5/56.6	25.1/56.1	61.4/73.2	63.0/74.1	63.4/74.6
RoPE-ViT	LLaMA	27.3/59.0	26.4/58.4	24.9/57.1	63.3/72.9	64.1/74.3	63.3/73.2
VMamba	Mamba-2	26.9/59.0	26.1/58.2	24.9/56.9	65.2/75.2	66.2/76.2	65.2/74.6
VMamba	Mamba-1	29.6/58.5	28.4/57.5	27.3/56.3	65.5/77.0	66.0/76.9	65.0/75.2

Table 3: **Resolution scaling on CLIP-Benchmark.** All models support arbitrary resolution inference. Both CLIMP variants demonstrate strong performance across all resolutions, achieving the best results on Acc@1 and retrieval metrics (IR@5/TR@5).

Vision Tower	Text Tower	224	512	896
FlexViT	LLaMA	54.3/56.7	52.2/52.7	41.3/37.6
NaFlex	LLaMA	58.5/64.2	58.0/60.4	49.9/46.4
RoPE-ViT	LLaMA	66.0/73.6	63.7/70.0	37.7/30.9
CLIMP (VMamba)	Mamba-2	<u>67.7/75.2</u>	<u>64.6/67.2</u>	<u>55.9/49.9</u>
CLIMP (VMamba)	Mamba-1	67.8/75.5	64.8/66.8	56.5/49.5

Table 4: **High-resolution retrieval.** Average Recall@5 (IR@5/TR@5) on NoCaps and Crossmodal-3600. Both CLIMP variants demonstrate strong performance across all resolutions, with the performance gap over transformer baselines widening substantially at 896×896.

et al., 2024), with SSM benefits most pronounced for natural distribution shifts.

4.3 High-Resolution

A key advantage of state-space models is native resolution flexibility. Unlike transformers, which require positional embedding interpolation (RoPE-ViT) or complex training (FlexViT, NaFlex) to handle varying input sizes, CLIMP generalizes to higher resolutions without architectural modifications or additional training. We demonstrate this by training all models at 224×224 and evaluating at up to 896×896 with no fine-tuning.

CLIP-Benchmark Evaluation. We evaluate on CLIP-Benchmark across resolutions from 224 to 384, limiting to 384×384 because over half of datasets have native resolutions below 384×384, making higher-resolution less meaningful.

Table 3 shows that at native 224×224 resolution, both CLIMP variants achieve the top two positions

Vision Tower	Text Tower	Flickr8k-R		DOCCI	
		I→T	T→I	I→T	T→I
FlexViT	LLaMA	75.0	79.0	42.8	36.3
NaFlex	LLaMA	80.2	86.8	55.3	53.4
ViT	LLaMA	82.0	85.8	—	—
RoPE-ViT	LLaMA	85.8	<u>93.6</u>	39.5	27.9
CLIMP (VMamba)	Mamba-2	<u>88.2</u>	92.6	62.6	51.7
CLIMP (VMamba)	Mamba-1	89.4	95.9	67.1	50.4

Table 5: **Recall@5 comparison on dense captioning retrieval benchmarks.** Flickr8k-Rephrased (Flickr8k-R) uses LLM-augmented captions (avg. 134 tokens); DOCCI contains naturally detailed descriptions (avg. 142 tokens). Both datasets have >94% of captions exceeding the 77-token context limit. Our CLIMP models consistently outperform transformer-based baselines, demonstrating effective retrieval with extended textual descriptions beyond CLIP’s token limit.

on retrieval. This advantage persists across all resolutions: at 320×320 and 384×384, both variants continue to occupy the top two positions on image and text recall. For classification, Mamba-1 achieves best Acc@1 across all resolutions, while RoPE-ViT and Mamba-2 compete for best Acc@5.

Scaling to Higher Resolutions. To rigorously evaluate resolution scaling, we test on NoCaps (Agrawal et al., 2019) (4.5K images, avg. 810×960) and Crossmodal-3600 (Thapliyal et al., 2022) (3.6K images, avg. 640×520) - benchmarks whose native resolutions exceed standard CLIP evaluation datasets. Table 4 shows average retrieval performance. Both CLIMP variants consistently outperform all baselines at every resolution, with the gap widening substantially at higher resolutions. At 896×896, CLIMP maintains strong performance while transformer baselines degrade significantly—achieving +18–19% advantage over RoPE-ViT on both image and text retrieval. Notably, both variants surpass FlexViT and NaFlex despite these models being specifically designed for arbitrary resolutions. See Table 11 for detailed results.

4.4 Dense Captioning Retrieval.

Complementary to our high-resolution evaluation, which tests robustness to out-of-distribution image sizes, we evaluate robustness to out-of-distribution text lengths. Our architecture overcomes CLIP’s fixed 77-token context window limitation. We evaluate on dense captioning tasks: (1) Flickr8k-test captions rephrased using LLaMA-3.3-70B (Touvron et al., 2023) (average 134 tokens, 98.3% exceeding 77 tokens), and (2) DOCCI (Onoe et al., 2024) with naturally verbose descriptions (average 142 tokens, 94.4% exceeding 77 tokens). As shown in Table 5, CLIMP variants consistently outperform all transformer baselines, achieving up to 3.6% improvement on Flickr8k-Rephrased and 11.8% on DOCCI, demonstrating superior retrieval with extended textual descriptions. Full results in Appendix Tables 12 and 13.

4.5 Analysis

4.5.1 Spatial Inductive Bias

To understand the source of VMamba’s advantages, we investigate its spatial inductive bias. Prior work has shown that locality bias benefits vision tasks by enabling more sample-efficient learning (d’Ascoli et al., 2021), a property ViTs lack due to their permutation-invariant attention. We validate this architectural difference using lightweight 3-layer VMamba (0.33M params) and ViT (0.35M params) models trained on CIFAR-10 (Krizhevsky and Hinton, 2009) with regular versus spatially distorted data with shuffled patch orders. VMamba achieves lower training loss on regular images, while ViT performs better on the distorted variant, confirming that SSM-based encoders encode sequential spatial structure as an inductive bias. Full results in Table 14 (Appendix).

4.5.2 Qualitative results

CLIMP also produces more interpretable image-text alignment maps. As shown in Figure 2, CLIMP correctly localizes the wooden deck and fence structure described in the caption, while RoPE-ViT and FlexViT exhibit diffuse attention scattered across irrelevant areas. Additional examples in Figure 5 (Appendix).

4.5.3 Representational Geometry Analysis

To understand CLIMP’s retrieval advantages, we analyze embedding geometry on NoCaps (Agrawal et al., 2019) following Wang & Isola (Wang and Isola, 2020), measuring *alignment* (matched

Vision Tower	Text Tower	Alignment \downarrow	Uniformity \downarrow		Hubness \downarrow	
			Image	Text	Image	Text
FlexViT	LLaMA	1.111	-2.87	-3.50	1.19	1.23
NaFlex	LLaMA	1.039	-3.30	-3.50	0.93	1.24
RoPE-ViT	LLaMA	1.052	-3.16	-3.52	1.04	1.25
CLIMP (VMamba)	Mamba-1	0.982	-3.18	-3.54	1.01	1.15
CLIMP (VMamba)	Mamba-2	1.000	-3.16	-3.54	1.01	1.13

Table 6: **Embedding geometry analysis on NoCaps.** We analyze alignment, uniformity, and hubness. CLIMP achieves better alignment and lower text hubness than transformer baselines, explaining its superior retrieval performance. \downarrow = lower is better for all metrics.

pairs should be close), *uniformity* (embeddings spread evenly on the hypersphere), and *hubness* (Radovanović et al., 2010)—the tendency for certain embeddings to dominate nearest-neighbor lists, degrading retrieval quality (Feldbauer and Flexer, 2019).

Table 6 shows that CLIMP achieves superior alignment and lower text hubness than transformer baselines. These properties explain CLIMP’s retrieval gains: better alignment improves matching accuracy, while reduced hubness benefits text retrieval and implies less reliance on spurious correlations, potentially contributing to improved OOD robustness (Section 4.2).

4.5.4 Memory and Computational Efficiency

Beyond representation quality, CLIMP also offers significant efficiency improvements. As shown in Figure 3, CLIMP requires 5 \times less resolution-specific memory (10.0 vs 50.4 MB) and 1.8 \times fewer FLOPs (259.7 vs 457.9 GFLOPs) than ViT variants at 896 \times 896, with the gap widening at higher resolutions due to Mamba’s linear complexity.

4.5.5 Scaling

We investigate how CLIMP scales with model size and training data.

Model Size. Table 7 shows ImageNet-1K zero-shot classification across model scales (22M–87M parameters). CLIMP consistently outperforms ViT-based alternatives across all sizes, with performance improving from 38.8% to 43.5% as model size increases.

Dataset Size. Figure 4 examines scaling with training data on Conceptual Captions. CLIMP exhibits a steep scaling curve that has not saturated, suggesting it would benefit from larger datasets.

4.6 Ablations

We ablate the text encoder contribution by replacing the LLM backbone while keeping the

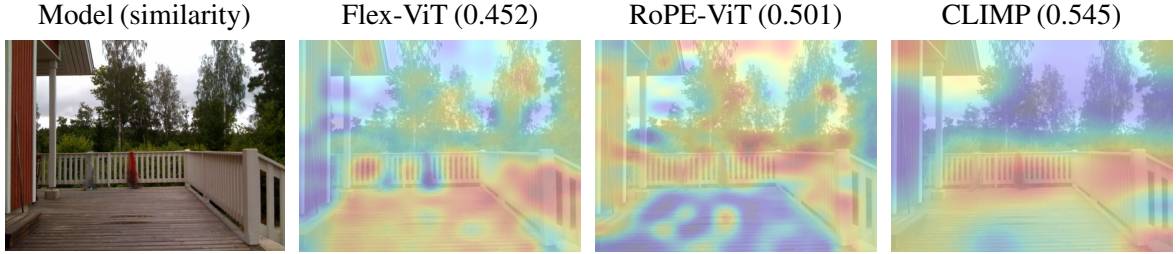


Figure 2: Visualization of Image-Text similarity for the caption: "A large porch with a wooden fence and no roof." CLIMP (similarity: 0.545) produces spatially coherent attention focused on the porch and fence, while RoPE-ViT (0.501) and FlexViT (0.452) show scattered, less interpretable patterns. Warmer colors indicate higher similarity.

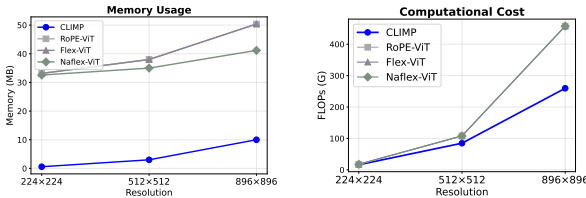


Figure 3: **Efficiency analysis.** CLIMP achieves superior memory and computational efficiency across all resolutions. (Left) Memory overhead is 4–57× lower. (Right) FLOPs scale linearly, yielding up to 1.8× reduction—a gap that widens with resolution.

Params	CLIMP (Mamba2)	FlexViT (LLaMA)	RoPE-ViT (LLaMA)
22-30M	38.8	32.5	33.2
50M	42.8	—	—
87M	43.5	38.3	40.7

Table 7: **Scaling behavior on ImageNet-1K zero-shot classification.** CLIMP consistently outperforms ViT-based alternatives across all scales, with performance improving steadily as model size increases.

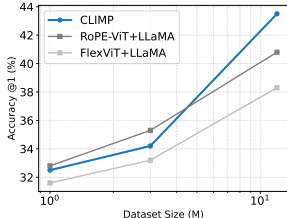


Figure 4: Scaling laws of CLIMP trained on CC dataset and evaluated on ImageNet-1K Acc@1. Performance improves consistently as training data scales from 1M to 12M samples.

vision encoder fixed. As shown in Table 8, the results reveal an architectural synergy: while RoPE-ViT shows minimal sensitivity to text encoder choice ($\pm 1\%$ across metrics), VMamba consistently benefits from Mamba-based text encoders, achieving +3.5% Acc@1 and +3.9% TR@5 over LLaMA. This suggests that while the vision encoder remains the primary driver of performance, matched SSM architectures in both modalities learn more compatible representations

Vision Tower	Text Tower	Acc@1/Acc@5	IR@5/TR@5
RoPE-ViT	LLaMA	27.27/58.95	63.35/72.93
RoPE-ViT	Mamba-2	27.42/58.69	62.59/72.99
RoPE-ViT	Mamba-1	28.10/58.54	63.17/74.28
RoPE-ViT	RoBERTa-L	27.47/58.64	64.82/74.72
RoPE-ViT	BERT-L	27.80/58.84	63.93/74.15
VMamba	LLaMA	26.13/57.30	63.21/73.16
VMamba	Mamba-2	26.94/ 59.04	65.17/75.25
VMamba	Mamba-1	29.59 /58.53	65.54 / 77.03

Table 8: **Architectural synergy.** We compare language model backbones across vision encoders. While RoPE-ViT shows minimal sensitivity to text encoder choice, VMamba consistently benefits from Mamba-based text encoders, suggesting that matched SSM architectures learn more compatible cross-modal representations.

for cross-modal alignment, providing additional justification for our fully SSM-based design.

5 Conclusions

We introduced CLIMP, the first contrastive vision-language Mamba model. By replacing ViT with VMamba and pairing it with Mamba LLMs, CLIMP achieves linear complexity in both modalities while producing superior representation quality and robustness. Our experiments reveal: (1) superior retrieval performance, driven by tighter cross-modal alignment and reduced hubness; (2) improved OOD robustness, notably surpassing CLIP-ViT-B/16 on ImageNet-O; (3) Memory and FLOPs reductions at high resolutions with native variable-resolution support; (4) Dense captioning retrieval beyond CLIP’s token limit; (5) spatial inductive bias contributing to sample-efficient learning.

These findings establish SSMs as a viable alternative to transformers for vision-language pre-training, overcoming limitations of CLIP implementations for high-resolution, memory-constrained, and long-context applications. Future directions include scaling to larger models and datasets, extending to generative vision-language tasks, and developing hybrid architectures (NVIDIA, 2025).

6 Limitations

Our experiments use CC12M (12M image-text pairs) with base-sized models ($\sim 86M$ parameters). While our scaling experiments suggest continued improvements, it remains to be verified whether CLIMP’s advantages persist at the scale of LAION-2B or ViT-L/H architectures.

References

Harsh Agrawal, Karan Desai, Yufei Wang, Xinlei Chen, Rishabh Jain, Mark Johnson, Dhruv Batra, Devi Parikh, Stefan Lee, and Peter Anderson. 2019. nocaps: novel object captioning at scale. In *Proceedings of the IEEE/CVF International Conference on Computer Vision*, pages 8948–8957.

Lucas Beyer, Pavel Izmailov, Alexander Kolesnikov, Mathilde Caron, Simon Kornblith, Xiaohua Zhai, Matthias Minderer, Michael Tschannen, Ibrahim Alabdulmohsin, and Filip Pavetic. 2023. Flexivit: One model for all patch sizes. In *Proceedings of the IEEE/CVF Conference on Computer Vision and Pattern Recognition*, pages 14496–14506.

Soravit Changpinyo, Piyush Sharma, Nan Ding, and Radu Soricut. 2021. Conceptual 12m: Pushing web-scale image-text pre-training to recognize long-tail visual concepts. In *Proceedings of the IEEE/CVF conference on computer vision and pattern recognition*, pages 3558–3568.

Mehdi Cherti and Romain Beaumont. 2025. [Clip benchmark](#).

Mehdi Cherti, Romain Beaumont, Ross Wightman, Mitchell Wortsman, Gabriel Ilharco, Cade Gordon, Christoph Schuhmann, Ludwig Schmidt, and Jenia Jitsev. 2023. Reproducible scaling laws for contrastive language-image learning. In *Proceedings of the IEEE/CVF Conference on Computer Vision and Pattern Recognition*, pages 2818–2829.

Tri Dao and Albert Gu. 2024. Transformers are SSMs: Generalized models and efficient algorithms through structured state space duality. In *Proceedings of the 41st International Conference on Machine Learning*, volume 235 of *Proceedings of Machine Learning Research*, pages 10041–10071. PMLR.

Stéphane d’Ascoli, Hugo Touvron, Matthew L Leavitt, Ari S Morcos, Giulio Biroli, and Levent Sagun. 2021. Convit: Improving vision transformers with soft convolutional inductive biases. In *International Conference on Machine Learning (ICML)*, pages 2286–2296.

Mostafa Dehghani, Basil Mustafa, Josip Djolonga, Jonathan Heek, Matthias Minderer, Mathilde Caron, Andreas Steiner, Joan Puigcerver, Robert Geirhos, Ibrahim Alabdulmohsin, and 1 others. 2024. Naflex: Training-free flexible image classification. *arXiv preprint arXiv:2406.04662*.

Jia Deng, Wei Dong, Richard Socher, Li-Jia Li, Kai Li, and Li Fei-Fei. 2009. Imagenet: A large-scale hierarchical image database. In *Proceedings of the IEEE/CVF Conference on Computer Vision and Pattern Recognition*, pages 248–255.

Jacob Devlin, Ming-Wei Chang, Kenton Lee, and Kristina Toutanova. 2019. [Bert: Pre-training of deep bidirectional transformers for language understanding](#). In *North American Chapter of the Association for Computational Linguistics*.

Alexey Dosovitskiy, Lucas Beyer, Alexander Kolesnikov, Dirk Weissenborn, Xiaohua Zhai, Thomas Unterthiner, Mostafa Dehghani, Matthias Minderer, Georg Heigold, Sylvain Gelly, Jakob Uszkoreit, and Neil Houlsby. 2021. [An image is worth 16x16 words: Transformers for image recognition at scale](#). In *International Conference on Learning Representations*.

Chengbin Du, Yanxi Li, and Chang Xu. 2024. Understanding robustness of visual state space models for image classification. *arXiv preprint arXiv:2403.10935*.

Alex Fang, Gabriel Ilharco, Mitchell Wortsman, Yuhao Wan, Vaishaal Shankar, Achal Dave, and Ludwig Schmidt. 2022. Data determines distributional robustness in contrastive language image pre-training (CLIP). In *International Conference on Machine Learning*, pages 6216–6234. PMLR.

Roman Feldbauer and Arthur Flexer. 2019. Adversarial hubness in multi-modal retrieval. In *International Conference on Similarity Search and Applications*, pages 169–176. Springer.

Albert Gu and Tri Dao. 2024. Mamba: Linear-time sequence modeling with selective state spaces. In *First conference on language modeling*.

Dan Hendrycks, Steven Basart, Norman Mu, Saurav Kadavath, Frank Wang, Evan Dorundo, Rahul Desai, Tyler Lixuan Zhu, Samyak Parajuli, Mike Guo, and 1 others. 2020. The many faces of robustness: A critical analysis of out-of-distribution generalization. 2021 ieee. In *CVF International Conference on Computer Vision (ICCV)*, volume 2.

Dan Hendrycks, Kevin Zhao, Steven Basart, Jacob Steinhardt, and Dawn Song. 2021. Natural adversarial examples. In *Proceedings of the IEEE/CVF conference on computer vision and pattern recognition*, pages 15262–15271.

Byeongho Heo, Song Park, Dongyoon Han, and Sangdoo Yun. 2024. Rotary position embedding for vision transformer. In *European Conference on Computer Vision (ECCV)*.

Weiquan Huang, Yifei Shen, and Yifan Yang. 2024. CLIP-Mamba: CLIP pretrained mamba models with OOD and hessian evaluation. *arXiv preprint arXiv:2404.19394*.

Chao Jia, Yinfei Yang, Ye Xia, Yi-Ting Chen, Zarana Parekh, Hieu Pham, Quoc Le, Yun-Hsuan Sung, Zhen Li, and Tom Duerig. 2021. Scaling up visual and vision-language representation learning with noisy text supervision. In *International Conference on Machine Learning*, pages 4904–4916. PMLR.

Alex Krizhevsky and Geoffrey Hinton. 2009. Learning multiple layers of features from tiny images. Technical report, University of Toronto.

Kunchang Li, Xinhao Li, Yi Wang, Yinan He, Yali Wang, Limin Wang, and Yu Qiao. 2024a. VideoMamba: State space model for efficient video understanding. In *European Conference on Computer Vision*, pages 237–255. Springer.

Qizhou Li, Weiran Huang, Jian Lin, Yanhong Zhong, and Lei Feng. 2024b. A sober look at the robustness of CLIPs to spurious features. *arXiv preprint arXiv:2403.11497*.

Yinhan Liu, Myle Ott, Naman Goyal, Jingfei Du, Mandar Joshi, Danqi Chen, Omer Levy, Mike Lewis, Luke Zettlemoyer, and Veselin Stoyanov. 2019. Roberta: A robustly optimized bert pretraining approach. *arXiv preprint arXiv:1907.11692*.

Yue Liu, Yunjie Tian, Yuzhong Zhao, Hongtian Yu, Lingxi Xie, Yaowei Wang, Qixiang Ye, Jianbin Jiao, and Yunfan Liu. 2024. VMamba: Visual state space model. In *Advances in Neural Information Processing Systems*, volume 37.

Hashmat Shadab Malik, Fahad Shamshad, Muzammal Naseer, Karthik Nandakumar, Fahad Shahbaz Khan, and Salman Khan. 2025. Towards evaluating the robustness of visual state space models. In *Proceedings of the Computer Vision and Pattern Recognition Conference*, pages 3544–3553.

NVIDIA. 2025. Nemotron 3 Nano: Open, efficient mixture-of-experts hybrid Mamba-Transformer model for Agentic reasoning. Technical report.

Yasumasa Onoe, Sunayana Rane, Zachary Berger, Yonatan Bitton, Jaemin Cho, Roopal Garg, Alexander Ku, Zarana Parekh, Jordi Pont-Tuset, Garrett Tanzer, Su Wang, and Jason Baldridge. 2024. DOCCI: Descriptions of Connected and Contrasting Images. In *ECCV*.

Badri N Patro and Vijay S Agneeswaran. 2024. Simba: Simplified mamba-based architecture for vision and multivariate time series. *arXiv preprint arXiv:2403.15360*.

Alec Radford, Jong Wook Kim, Chris Hallacy, Aditya Ramesh, Gabriel Goh, Sandhini Agarwal, Girish Sastry, Amanda Askell, Pamela Mishkin, Jack Clark, Gretchen Krueger, and Ilya Sutskever. 2021. Learning transferable visual models from natural language supervision. In *Proceedings of the 38th International Conference on Machine Learning*, volume 139 of *Proceedings of Machine Learning Research*, pages 8748–8763. PMLR.

Miloš Radovanović, Alexandros Nanopoulos, and Mirjana Ivanović. 2010. Hubs in space: Popular nearest neighbors in high-dimensional data. *Journal of Machine Learning Research*, 11:2487–2531.

Benjamin Recht, Rebecca Roelofs, Ludwig Schmidt, and Vaishaal Shankar. 2019. Do imagenet classifiers generalize to imagenet? In *International conference on machine learning*, pages 5389–5400. PMLR.

Jiacheng Ruan and Suncheng Xiang. 2024. VM-UNet: Vision mamba UNet for medical image segmentation. *arXiv preprint arXiv:2402.02491*.

Christoph Schuhmann, Romain Beaumont, Richard Vencu, Cade Gordon, Ross Wightman, Mehdi Cherti, Theo Coombes, Aarush Katta, Clayton Mullis, Mitchell Wortsman, and 1 others. 2022. Laion-5b: An open large-scale dataset for training next generation image-text models. *Advances in neural information processing systems*, 35:25278–25294.

Christoph Schuhmann, Richard Vencu, Romain Beaumont, Robert Kaczmarczyk, Clayton Mullis, Aarush Katta, Theo Coombes, Jenia Jitsev, and Aran Komatsuzaki. 2021. Laion-400m: Open dataset of clip-filtered 400 million image-text pairs. *arXiv preprint arXiv:2111.02114*.

Jianlin Su, Murtadha Ahmed, Yu Lu, Shengfeng Pan, Wen Bo, and Yunfeng Liu. 2024. Roformer: Enhanced transformer with rotary position embedding. *Neurocomputing*, 568:127063.

Quan Sun, Yuxin Fang, Ledell Wu, Xinlong Wang, and Yue Cao. 2023. EVA-CLIP: Improved training techniques for CLIP at scale. *arXiv preprint arXiv:2303.15389*.

Camilo Tamayo-Rousseau, Yunjia Zhao, Yiqun Zhang, and Randall Balestrieri. 2025. Your attention matters: to improve model robustness to noise and spurious correlations. *arXiv preprint arXiv:2507.20453*.

Rohan Taori, Achal Dave, Vaishaal Shankar, Nicholas Carlini, Benjamin Recht, and Ludwig Schmidt. 2020. Measuring robustness to natural distribution shifts in image classification. In *Advances in Neural Information Processing Systems*, volume 33, pages 18583–18599.

Ashish Thapliyal, Jordi Pont-Tuset, Xi Chen, and Radu Soricut. 2022. Crossmodal-3600: A Massively Multilingual Multimodal Evaluation Dataset. In *EMNLP*.

Hugo Touvron, Thibaut Lavril, Gautier Izacard, Xavier Martinet, Marie-Anne Lachaux, Timothée Lacroix, Baptiste Rozière, Naman Goyal, Eric Hambro, Faisal Azhar, and 1 others. 2023. Llama: Open and efficient foundation language models. *arXiv preprint arXiv:2302.13971*.

Michael Tschanne, Alexey Gritsenko, Xiao Wang, Muhammad Ferjad Naeem, Ibrahim Alabdulmohsin, Nikhil Parthasarathy, Talfan Evans, Lucas Beyer, Ye Xia, Basil Mustafa, and 1 others. 2025. SigLIP 2: Multilingual vision-language encoders with improved semantic understanding, localization, and dense features. *arXiv preprint arXiv:2502.14786*.

Haohan Wang, Songwei Ge, Zachary Lipton, and Eric P Xing. 2019. Learning robust global representations by penalizing local predictive power. *Advances in neural information processing systems*, 32.

Tongzhou Wang and Phillip Isola. 2020. Understanding contrastive representation learning through alignment and uniformity on the hypersphere. In *International Conference on Machine Learning*, pages 9929–9939. PMLR.

Hu Xu, Saining Xie, Xiaoqing Ellen Tan, Po-Yao Huang, Russell Howes, Vasu Sharma, Shang-Wen Li, Gargi Ghosh, Luke Zettlemoyer, and Christoph Feichtenhofer. 2024. Demystifying CLIP data. In *International Conference on Learning Representations*.

Xiaohua Zhai, Basil Mustafa, Alexander Kolesnikov, and Lucas Beyer. 2023. Sigmoid loss for language image pre-training. In *Proceedings of the IEEE/CVF International Conference on Computer Vision*, pages 11975–11986.

Jiuming Zhang, Guoqing Liu, Xingye Ma, Chaoda Liu, and Cheng Zhou. 2024. Point mamba: A novel point cloud backbone based on state space model with octree-based ordering strategy. *arXiv preprint arXiv:2403.06467*.

Yuqing Zhou and Ziwei Zhu. 2025. Fighting spurious correlations in text classification via a causal learning perspective. In *Proceedings of the 2025 Conference of the Nations of the Americas Chapter of the Association for Computational Linguistics: Human Language Technologies (Volume 1: Long Papers)*, pages 4264–4274.

Lianghui Zhu, Bencheng Liao, Qian Zhang, Xinlong Wang, Wenyu Liu, and Xinggang Wang. 2024. Vision mamba: Efficient visual representation learning with bidirectional state space model. In *Proceedings of the 41st International Conference on Machine Learning*, volume 235 of *Proceedings of Machine Learning Research*, pages 62429–62442. PMLR.

Itamar Zimerman and Lior Wolf. 2024. Viewing transformers through the lens of long convolutions layers. In *Forty-first International Conference on Machine Learning*.

A Appendix

A.1 Similarity Visuals

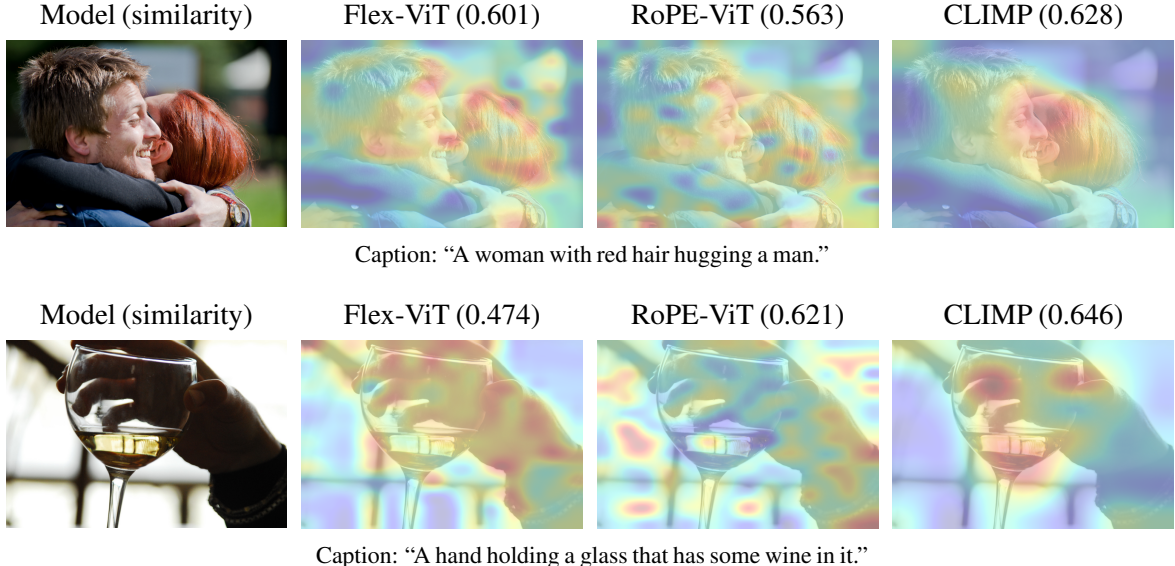


Figure 5: Visualization of image-text similarity. CLIMP exhibits more interpretable alignment and better similarity performance.

A.2 Main Results

Dataset	ViT-B-P-16+LLaMA		VMamba-B+Mamba2		VMamba-B+Mamba1		RoPE-ViT-B+LLaMA		Flex-ViT-B+LLaMA		NaFlex-ViT-B+LLaMA	
	Acc@1	Acc@5	Acc@1	Acc@5	Acc@1	Acc@5	Acc@1	Acc@5	Acc@1	Acc@5	Acc@1	Acc@5
cars	8.9	30.4	9.9	34.1	9.1	32.4	8.4	31.1	8.3	31.0	8.5	30.4
country211	4.7	17.0	4.7	15.8	4.3	15.4	3.9	14.5	4.1	14.9	4.2	14.7
fer2013	35.9	85.0	22.2	83.1	18.8	81.7	29.1	86.9	15.1	77.2	15.2	76.6
fgvc_aircraft	1.3	6.2	2.4	9.9	2.5	9.7	1.7	8.6	2.6	9.4	1.9	8.3
imagenet-a	13.9	37.6	15.5	45.5	15.6	45.3	16.3	46.3	13.2	41.2	12.0	36.0
imagenet-o	27.7	55.8	48.1	77.0	49.8	78.8	40.1	69.8	38.0	68.2	38.5	67.6
imagenet-r	42.9	69.7	46.2	74.4	46.6	74.5	47.8	76.0	45.4	74.3	44.8	72.5
imagenet1k	36.0	64.9	43.5	73.9	44.0	74.8	40.7	71.5	38.3	69.0	36.6	67.0
imagenet_sketch	21.7	46.1	27.0	54.2	27.5	54.4	27.4	53.1	24.6	50.0	23.5	49.1
imagenetv2	30.0	57.5	37.0	67.6	37.5	68.4	34.4	65.4	32.8	62.5	31.4	60.5
objectnet	23.6	46.7	29.2	55.9	28.1	54.3	33.1	60.9	28.1	54.3	26.8	53.4
sun397	53.2	86.7	49.5	84.6	48.2	84.2	47.5	83.2	49.1	83.7	48.8	83.6
voc2007	77.9	96.7	69.4	93.9	75.8	96.2	71.2	92.2	65.4	88.9	68.3	91.5
cifar100	66.3	91.4	50.7	82.8	48.3	81.1	54.5	84.4	54.3	83.2	51.4	82.1
cifar10	94.2	99.9	84.8	99.5	83.0	99.4	88.4	99.4	83.1	98.4	83.1	98.9
clevr_closest_object_distance	18.7	75.5	16.8	91.9	18.3	90.9	16.4	93.9	15.9	91.5	16.1	91.9
clevr_count_all	19.8	65.5	13.1	71.0	16.2	63.8	17.1	70.4	13.8	63.4	14.7	64.7
diabetic_retinopathy	2.3	100.0	10.4	100.0	71.3	100.0	3.5	100.0	12.7	100.0	30.7	100.0
dmlab	14.4	83.4	15.2	85.1	17.8	81.2	20.4	82.1	21.2	84.8	11.9	81.4
dsprites_label_orientation	2.1	9.9	2.8	13.7	2.8	11.5	2.6	13.3	2.7	13.0	2.1	11.8
dsprites_label_x_position	3.2	15.4	2.9	15.2	3.2	15.6	3.1	15.4	3.1	15.3	3.1	15.5
dsprites_label_y_position	3.2	15.5	3.1	15.8	3.4	16.2	3.1	15.0	2.9	14.3	3.2	15.6
smallnorb_label_azimuth	4.8	28.7	5.7	27.4	5.1	27.0	5.4	28.0	5.1	27.6	5.1	28.6
smallnorb_label_elevation	12.9	60.4	10.8	55.6	10.3	54.2	10.9	54.7	9.9	54.7	12.0	58.5
svhn	17.0	64.0	9.8	48.1	9.9	52.3	7.0	57.7	20.8	62.9	9.4	55.4

Table 9: Zero-shot Classification Results. We report Top-1 (Acc@1) and Top-5 (Acc@5) accuracy (%) across various benchmarks.

Dataset	ViT-B-P-16+LLaMA		VMamba-B+Mamba2		VMamba-B+Mamba1		RoPE-ViT-B+LLaMA		Flex-ViT-B+LLaMA		NaFlex-ViT-B+LLaMA	
	T-R@5	I-R@5	T-R@5	I-R@5	T-R@5	I-R@5	T-R@5	I-R@5	T-R@5	I-R@5	T-R@5	I-R@5
flickr30k	82.7	72.9	85.0	76.9	87.5	76.5	82.9	73.9	81.9	72.8	81.1	72.1
flickr8k	78.4	68.1	79.3	69.1	81.7	70.5	77.6	68.1	77.0	66.6	81.5	66.0
mscoco_captions	57.5	47.3	61.4	49.5	61.9	49.6	58.3	48.1	58.1	47.7	57.1	46.3

Table 10: Zero-shot Retrieval Results. We report Text Retrieval Recall@5 (T-R@5) and Image Retrieval Recall@5 (I-R@5) (%) on standard retrieval benchmarks.

A.3 High-Resolution Detailed Results

Vision	Text	NoCaps				Crossmodal-3600					
		224	512	896	224	512	896	I→T	T→I	I→T	T→I
RoPE-ViT	LLaMA	67.6	78.9	65.1	75.9	38.6	34.9	64.4	68.2	62.3	64.1
NaFlex	LLaMA	60.4	69.1	59.7	65.0	51.6	50.8	56.7	59.3	56.3	55.7
FlexViT	LLaMA	56.0	62.9	53.4	57.8	42.2	41.2	52.6	50.5	50.9	47.6
VMamba	Mamba-2	70.2	81.3	66.4	72.4	57.1	53.8	65.2	69.2	62.8	61.9
VMamba	Mamba-1	70.5	81.9	66.9	72.7	57.1	53.5	65.1	69.1	62.6	60.8
											54.7
											46.0

Table 11: Retrieval performance (Recall@5) on NoCaps (Agrawal et al., 2019) and Crossmodal-3600 (Thapliyal et al., 2022) at different resolutions.

A.4 Dense Captioning Retrieval

Vision Tower	Text Tower	Image Retrieval			Text Retrieval		
		R@1	R@5	R@10	R@1	R@5	R@10
FlexViT	LLaMA	46.4	75.0	84.5	55.7	79.0	87.8
NaFlex	LLaMA	50.9	80.2	88.9	66.1	86.8	93.8
ViT	LLaMA	53.9	82.0	90.1	64.8	85.8	92.0
RoPE-ViT	LLaMA	60.7	85.8	93.3	77.6	93.6	97.0
VMamba	Mamba-2	63.3	88.2	94.6	75.7	92.6	96.2
VMamba	Mamba-1	67.0	89.4	94.7	81.3	95.9	98.4

Table 12: Zero-shot retrieval on rephrased Flickr8k-test with dense captions. Captions were rephrased using an LLM (avg. 134 tokens vs. original 14), with 98.32% exceeding the 77-token limit. Images resized to 224×224.

Vision Tower	Text Tower	Image Retrieval			Text Retrieval		
		R@1	R@5	R@10	R@1	R@5	R@10
RoPE-ViT	LLaMA	18.0	39.5	50.5	10.5	27.9	38.1
FlexViT	LLaMA	20.5	42.8	53.8	15.6	36.3	47.6
NaFlex	LLaMA	29.1	55.3	67.5	26.1	53.4	65.1
VMamba	Mamba-2	33.4	62.6	74.0	24.6	51.7	63.7
VMamba	Mamba-1	37.3	67.1	77.8	23.8	50.4	62.7

Table 13: Zero-shot retrieval on DOCCI (Onoe et al., 2024), a dense captioning dataset with long descriptions (avg. 142 tokens, 94.4% exceeding 77 tokens). Images resized to 896×896.

A.5 VMamba’s Inductive Bias

Model	Data	Train Loss	Test Acc.
VMamba	Regular	1.028	69.33
ViT	Regular	1.121	67.50
VMamba	Shuffled	1.612	46.44
ViT	Shuffled	1.328	59.72

Table 14: Spatial inductive bias analysis. We train lightweight 3-layer VMamba (0.33M params) and ViT (0.35M params) on CIFAR-10 with regular and shuffled patch orders. VMamba achieves lower training loss on regular images but degrades significantly under shuffling, while ViT shows the opposite pattern—performing relatively better on distorted data. This confirms that SSM-based encoders rely on sequential spatial structure as an inductive bias.



Figure 6: Visualization of the original and distorted CIFAR-10 samples